Progress in Nuclear Energy 165 (2023) 104898

Contents lists available at ScienceDirect

Progress in Nuclear Energy

journal homepage: www.elsevier.com/locate/pnucene

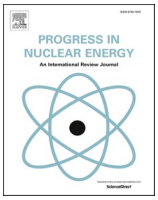

Comparison of Raman and mid-infrared spectroscopy for quantification of nitric acid in PUREX-relevant mixtures

Catriona McFarlan [a], Alison Nordon [a,*], Mark Sarsfield [b], Robin Taylor [b], Hongyan Chen [c]

[a] WestCHEM, Department of Pure and Applied Chemistry and the Centre for Process Analytics and Control Technology, University of Strathclyde, 295 Cathedral Street, Glasgow, G1 1XL, UK
[b] National Nuclear Laboratory, Central Laboratory, Sellafield, Seascale, Cumbria, CA20 1PG, UK
[c] School of Chemical Engineering and Analytical Science, University of Manchester, Oxford Road, Manchester, M13 9PL, UK

ARTICLE INFO

Keywords:
Nitric acid
Liquid-liquid extraction
Process analysis
Raman spectroscopy
Mid-infrared spectroscopy
Chemometrics

ABSTRACT

During the plutonium uranium reduction extraction (PUREX) process, nitric acid facilitates the extraction of actinides from the aqueous phase into the organic phase by forming neutral, organic soluble complexes with tri-*n*-butyl phosphate (TBP). The concentration of nitric acid is generally measured by titration; however, titration is a time-consuming method that generates significant volumes of additional waste. Optical spectroscopic techniques can be used to perform fast, automated measurements off-line or on-line, without generating any waste. In this work, the effectiveness of Raman and mid-infrared (MIR) spectroscopy has been compared for the first time as an alternative to titration for the quantification of nitric acid in PUREX-relevant mixtures. Samples of 0–12 M nitric acid in the aqueous phase and 0–1.10 M nitric acid in the organic phase (TBP/odourless kerosene (OK)–H_2O–HNO_3 model system) were analysed and partial least squares (PLS) regression models were built to predict nitric acid concentration. MIR spectra required less pre-processing than Raman spectra and more accurate predictions of nitric acid concentration were obtained for MIR spectroscopy than for Raman spectroscopy, with root mean square error of prediction (RMSEP) values of 0.099 M versus 0.148 M obtained for the aqueous phase and root mean square error of cross validation (RMSECV) values of 0.006 M versus 0.013 M obtained for the organic phase. To investigate the ability to predict nitric acid concentration in the presence of uranyl nitrate, samples containing uranium (0–100 g/L) and nitric acid (0.15–0.64 M) in the organic phase (U-TBP/OK-H_2O–HNO_3 model system) were analysed by Raman and MIR spectroscopy. The RMSECV was 0.027 M and 0.066 M for MIR and Raman spectroscopy, respectively; these values are higher than those obtained in the absence of uranyl nitrate owing to differences in the experimental approaches employed. Therefore, the results obtained demonstrate that MIR or Raman spectroscopy could be used to measure the concentration of nitric acid in the organic and aqueous phases in the PUREX process.

1. Introduction

The plutonium uranium reduction extraction (PUREX) process is a common industrial method for the extraction of plutonium and uranium (and sometimes neptunium (Taylor et al., 2013)) from spent nuclear fuel for recycling into new fuel (Debus et al., 2015; Herbst et al., 2011; Rodriguez-Ruiz et al., 2018). It is based on a liquid-liquid solvent extraction, with 20–30% v/v tri-*n*-butyl phosphate (TBP) in a hydrocarbon-based diluent as the organic phase, and nitric acid as the aqueous phase (Asmussen et al., 2019; Herbst et al., 2011; May et al., 1999). Nitric acid facilitates the extraction of actinides from the aqueous phase into the organic phase by forming neutral, organic soluble complexes with TBP (e.g. $UO_2(NO_3)_2$ $(TBP)_2$), and TBP can also be extracted alone as a complex with nitric acid, as shown in Equation (1) (Asmussen et al., 2019; Nelson et al., 2018). In addition to HNO_3·TBP, other $nHNO_3$·mTBP complexes such as $2HNO_3$·TBP and HNO_3·2 TBP can form (Balasubramonian et al., 2013).

$$HNO_3 + TBP \rightleftharpoons HNO_3{\cdot}TBP \quad (1)$$

The concentration of nitric acid can affect the extraction efficiency (Casella et al., 2013), so the ability to measure acid concentration is important. Nitric acid concentration is generally measured by titration, which can be time-consuming and generates significant volumes of

* Corresponding author.
E-mail address: alison.nordon@strath.ac.uk (A. Nordon).

https://doi.org/10.1016/j.pnucene.2023.104898
Received 26 May 2023; Received in revised form 5 August 2023; Accepted 7 September 2023
Available online 26 September 2023

additional radioactive waste. Optical spectroscopy is an alternative method, enabling the acquisition of fast, automated measurements with no additional waste generation. The use of fibre-coupled probes or flow cells allows the instruments to be located away from harsh, radioactive analytes (Bryan et al., 2011a; Schwantes et al., 2012). Optical spectroscopy can also be employed on-line enabling real-time monitoring for detection of deviations from expected conditions during the PUREX process and process control (Bryan et al., 2011a; Kirsanov et al., 2013). It could also be used to confirm that the concentration of nitric acid fed into the process is correct, which avoids the hazards associated with potential misrouting of material for off-line analysis.

Raman spectroscopy is the most commonly used optical spectroscopic technique for the analysis of nitric acid in PUREX-relevant mixtures, and a number of examples have been demonstrated (Arrigo et al., 2009; Asmussen et al., 2019; Bryan et al., 2011a, 2011b, 2011c, 2014; Casella et al., 2013, 2016; Lines et al., 2018; Nee et al., 2018; Nelson et al., 2018, 2019). Measurements are generally performed *in situ* using fibre-coupled probes, and the use of non-contact probes allows non-invasive measurements to be performed. Mid-infrared (MIR) spectroscopy is particularly suited to the analysis of the organic phase, due to the presence of the IR active phosphate group in TBP. However, it has not been employed for analysis of PUREX-relevant samples in the aqueous phase. The majority of examples in the literature are off-line studies of the organic phase (Borkowski et al., 2002; Chiarizia et al., 2003; Ferraro et al., 2001; Verma et al., 2018). MIR spectrometers are less easily installed in harsh process environments than Raman spectrometers owing to difficulties associated with transmitting MIR light through long lengths of optical fibre. However, *in situ* analysis is possible using attenuated total reflectance (ATR) probes coupled with shorter waveguides (<5 m) (Levitskaia et al., 2013), and a rugged MIR spectrometer attached directly to an ATR probe has been developed for use in industrial environments (Liu et al., 2019).

This paper presents the first comparison of the effectiveness of Raman and MIR spectroscopy for quantification of nitric acid during the PUREX process, as an alternative to titration. Raman and MIR spectroscopy were employed in conjunction with chemometrics to quantify nitric acid concentrations in the aqueous and organic phases of a PUREX-relevant model system, TBP/odourless kerosene (OK)–H_2O–HNO_3. The presence of uranyl nitrate in the PUREX process may impact the ability to predict nitric acid concentration, so the effectiveness of Raman and MIR spectroscopy for quantification of nitric acid in the organic phase of a U-TBP/OK-H_2O–HNO_3 model system was also explored.

2. Material and methods

2.1. Sample preparation

2.1.1. TBP/OK-H_2O–HNO_3 model system

Ten aqueous phase samples of nitric acid were prepared at the University of Strathclyde, at concentrations of 0, 0.5, 1, 2, 3, 4, 5, 6, 9 and 12 M (see Table S1 in the Supplementary Information), chosen based on the range relevant to the PUREX process (Asmussen et al., 2019). The samples were prepared by mass, using a stock solution of 70% nitric acid (≥68% and ≤72%, Fisher Scientific, Loughborough, UK). The exact concentration of the stock solution was measured by titration, as detailed in section 2.2.

An additional set of ten nitric acid samples in the aqueous phase were prepared at the same concentrations (see Table S2 in the Supplementary Information), for extraction into an organic solvent consisting of 30% v/v TBP (≥99.0%, Sigma Aldrich, Darmstadt, Germany) in odourless kerosene (OK) (Exxsol™ D80 obtained from a UK-based operational reprocessing plant). Prior to extraction, the solvent was washed by contacting sequentially with the following aqueous reagents to remove impurities.

1 0.1 M HNO_3 at a solvent:aqueous reagent (S/A) ratio of 1:1 for 15 min
2 1 M Na_2CO_3 at S/A ratio of 2:1 for 10 min
3 1 M NaOH at S/A ratio of 2:1 for 10 min
4 0.1 M HNO_3 at S/A ratio of 1:1 for 10 min

Each aqueous phase sample was transferred to a centrifuge tube and mixed with the TBP/OK solvent in a 1:1 ratio at room temperature (based on the ratio and temperatures given in the literature (Asmussen et al., 2019; Borkowski et al., 2002; Chiarizia et al., 2003; Lefebvre et al., 2017; Levitskaia et al., 2013)) for 15 min using a Fisherbrand™ ZX4 IR vortex mixer at 2350 rpm (Asmussen et al., 2019). The aqueous and organic phases were then separated by centrifugation (Arrigo et al., 2009; Borkowski et al., 2002; Bryan et al., 2014; Casella et al., 2013; Orton et al., 2011; Schwantes et al., 2012), using an Ohaus Frontier 5706 centrifuge at 6000 rpm for 2 min.

The nitric acid concentration in the aqueous phase post-extraction was determined by titration, as described in section 2.2. The nitric acid concentration in the organic phase post-extraction was calculated based on a model for nitric acid extraction into TBP (McLachlan et al., 2016). The initial and post-extraction concentrations of nitric acid in each sample are given in Table 1.

2.1.2. U-TBP/OK-H_2O–HNO_3 model system

To investigate the ability to predict nitric acid concentration in the presence of uranyl nitrate, thirteen samples containing uranium and nitric acid in the organic phase were prepared at NNL. Four stock aqueous phase samples were first prepared, containing 3.50 M nitric acid and target uranium concentrations of 30, 60, 90 and 140 g/L. The uranium and nitric acid in these samples were extracted into 20–40% v/v TBP in OK to produce thirteen samples with uranium concentrations ranging from 0 to 100 g U/L (with uranium present as U(VI) in the form $UO_2(NO_3)_2$) and TBP concentrations ranging from 20 to 40% v/v, in a central composite design. The composition of the samples is given in Table S3 of the Supplementary Information. The uranium concentrations post-extraction were determined using ultraviolet–visible (UV–vis) spectroscopy, as described in the Supplementary Information. Nitric acid concentrations were calculated based on a model for nitric acid extraction into TBP in the presence of uranium (Chen et al., 2016), and ranged from 0.15 to 0.64 M.

2.2. Titration

To determine the concentration of nitric acid present in the samples detailed in section 2.1.1, all titrations were performed using a Mettler Toledo EasyPlus Easy pH autotitrator. The minimum sample volume required to ensure that the electrode was sufficiently submerged in the solution was 45 mL. Therefore, all samples were diluted to 100 mL, and

Table 1
Initial and post-extraction concentrations of nitric acid in each sample. Post-extraction concentrations in the aqueous phase were measured by titration and post-extraction concentrations in the organic phase were calculated based on a model for nitric acid extraction into TBP (McLachlan et al., 2016).

Sample	Initial nitric acid concentration/M	Post-extraction nitric acid concentration in aqueous phase/M	Post-extraction nitric acid concentration in organic phase/M
1	0.00	0.00	0.00
2	0.50	0.43	0.05
3	1.00	0.84	0.15
4	2.00	1.66	0.36
5	2.98	2.49	0.54
6	3.98	3.34	0.69
7	4.98	4.24	0.83
8	5.99	5.24	0.93
9	8.96	8.23	1.07
10	11.94	11.26	1.10

45–50 mL aliquots were used for titration. Dilution factors were calculated to allow each sample to be neutralised with roughly half the volume of the 20 mL burette.

To determine the exact concentration of the 70% nitric acid stock solution, three aliquots were diluted by a factor of 25 and titrated with 1 M sodium hydroxide (≥0.999 M and ≤1.001 M NIST standard solution, Fisher Scientific, Loughborough, UK). The concentrations obtained are displayed in Table S4 of the Supplementary Information, and the average value, 15.69 M, was used to calculate the actual nitric acid concentration of each aqueous phase sample (see Tables S1 and S2 in the Supplementary Information).

Each aqueous phase sample post-extraction was diluted to 100 mL with deionised water by a factor of either 10, 20 or 25. To determine appropriate dilution factors for titration of the aqueous phase samples post-extraction, estimates of the expected nitric acid concentrations in the organic phase post-extraction were calculated using Equation (2) (Asmussen et al., 2019), where $[HNO_{3\ (org)}]$ is the concentration of nitric acid in the organic phase post-extraction, $[TBP]_{initial}$ is the initial molar concentration of TBP in the organic phase and $a_{HNO_{3\ (aq)}}$ is the chemical activity of nitric acid in the aqueous phase. $a_{HNO_{3\ (aq)}}$ was derived by multiplying the activity coefficients of the undissociated acid (Davis and Debruin, 1964) with the molality of the acid (Asmussen et al., 2019). Estimates of the expected nitric acid concentrations in the aqueous phase post-extraction were then calculated by subtraction of the organic phase estimations from the initial concentrations (Table S2); these estimates are displayed in Table S5 of the Supplementary Information.

$$\left[HNO_{3\ (org)}\right] = \frac{0.16 \times a_{HNO_{3\ (aq)}} \times [TBP]_{initial}}{1 + 0.16 \times a_{HNO_{3\ (aq)}}} \quad (2)$$

Samples 2 and 3 were titrated with 0.1 M sodium hydroxide (≥0.0999 M and ≤0.1001 M NIST standard solution, Fisher Scientific, Loughborough, UK), and samples 4–10 were titrated with 1 M sodium hydroxide (≥0.999 M and ≤1.001 M NIST standard solution, Fisher Scientific, Loughborough, UK). Two batches of each sample were prepared where possible and for all samples, two titrations of the first batch were performed. 50 mL of diluted sample was used for the first titration of each batch, and 45 mL was used for the second (as a small amount of the initial 100 mL was lost due to residue when transferring the sample between the volumetric flask, storage bottle and pipette, so it was not possible to measure exactly 50 mL twice). The concentrations measured by titration are displayed in Table 2, along with the average concentration for each sample across all measurements. The average concentrations were used to build the partial least squares (PLS) models detailed in section 2.4.

To confirm that the measurements obtained by the autotitrator were accurate, the concentrations of a subset of the initial aqueous phase samples detailed in section 2.1.1 (samples 2, 5, 8 and 10) were also determined by titration using the same procedure. The results for samples 8 and 10 were within 0.1 M of the expected concentrations, and the results for samples 2 and 5 were within 0.015 M of the expected concentrations, confirming the accuracy of the procedure.

2.3. Spectroscopic analysis

2.3.1. TBP/OK-H_2O/HNO_3 model system

The ten aqueous phase samples of nitric acid detailed in section 2.1.1 were analysed by Raman and MIR spectroscopy at the University of Strathclyde. Three repeat measurements of each sample were acquired and all measurements, including the repeats, were performed in a random order. The Raman measurements were performed using a Kaiser RXN1 spectrometer with a laser wavelength of 785 nm and a spectral range of 175–1875 cm^{-1}. The spectrometer was coupled to a non-contact PhAT probe with a 6 mm diameter laser spot. The samples were contained in glass bottles and measurements were made through the side of the bottle. An exposure time of 15 s was used, and each measurement was an average of four scans. MIR measurements were conducted using an ABB MB3000 spectrometer, which was fibre-coupled to a diamond ATR probe (12 mm diameter) with a hastelloy body (Art Photonics, Germany). Spectra were acquired over the range 600–1900 cm^{-1} using an air background. For each measurement, the fibre-coupled probe was inserted into the sample and 16 scans were acquired at a resolution of 16 cm^{-1}. The aqueous and organic phase samples post-extraction were analysed by Raman and MIR spectroscopy using the same procedure. For the MIR measurements of the organic phase samples, a resolution of 2 cm^{-1} was used to distinguish peaks arising from molecularly similar species.

2.3.2. U-TBP/OK-H_2O–HNO_3 model system

The samples containing uranyl nitrate and nitric acid (detailed in section 2.1.2) were analysed by Raman and MIR spectroscopy at NNL. The Raman measurements were performed using a micro-Raman Renishaw InVia Qontor Spectrometer System, with a 633 nm laser and a fibre-coupled probe. The samples were contained in glass vials and measurements were made through the glass. An exposure time of 1 s was used and each measurement consisted of 100 accumulations, covering a spectral range of 388–1552 cm^{-1}. The MIR spectrometer operated in the region 350–6000 cm^{-1}, and an Agilent Cary 630 FTIR diamond ATR crystal accessory was used to perform the measurements.

2.4. Data analysis

2.4.1. TBP/OK-H_2O/HNO_3 model system

For the nitric acid samples detailed in section 2.1.1, PLS regression was used to predict the concentration of nitric acid in the aqueous and organic phases post-extraction. PLS regression was performed using PLS Toolbox version 8.6.2 (Eigenvector, Washington, USA) in MATLAB 2016b (MathWorks, Massachusetts, USA). The details of the models built are given in Table 3. For the aqueous phase, the initial set of ten samples (detailed in section 2.1.1) was used as the calibration set, and the post-extraction samples were used as the test set. For the organic phase, the models were built and tested using a single set of samples. The number of latent variables to include in each model was chosen by cross validation. This involved building PLS models leaving out blocks of

Table 2
Concentration of nitric acid in the aqueous phase samples post-extraction, measured by titration. Expected concentrations were calculated using Equation (2), and average measured concentrations were calculated using all measurements for each sample across batches 1 and 2.

Sample	Expected concentration/M	Batch 1 concentration/M	Batch 1 repeat concentration/M	Batch 2 concentration/M	Average measured concentration/M
1	0.00	N/A	N/A	N/A	N/A
2	0.41	0.43	0.43	0.43	0.43
3	0.80	0.84	0.85	0.84	0.84
4	1.59	1.66	1.67	N/A	1.66
5	2.38	2.48	2.49	N/A	2.49
6	3.23	3.33	3.35	3.34	3.34
7	4.11	4.23	4.28	4.21	4.24
8	5.05	5.21	5.25	5.27	5.24
9	7.91	8.21	8.24	8.24	8.23
10	10.86	11.21	11.30	11.27	11.26

Table 3
Parameters used to build PLS models for the prediction of nitric acid concentration, and RMSEP and/or RMSECV values obtained for each model. MC = mean centring and norm = normalisation to unit length. Concentrations ranged from 0 to 12 M in the aqueous phase and 0 to 1.10 M in the organic phase.

Model	Technique	Spectral range/ cm^{-1}	Pre-processing	Calibration samples	Test samples	Latent variables	RMSEC/ M	RMSEP/ M	RMSECV/ M
1	Raman	500–1500	1st derivative, MC	Aqueous	Aqueous post-extraction	3	0.163	0.627	0.251
2	Raman	500–1500	1st derivative, norm, MC	Aqueous	Aqueous post-extraction	2	0.071	0.246	0.076
1 & 2	Raman	500–1500	1st derivative, MC (<2 M) 1st derivative, norm, MC (≥2 M)	Aqueous	Aqueous post-extraction	3 (<2 M) & 2 (≥2 M)	0.055	0.148	0.060
3	Raman	500–1500	1st derivative, MC	Organic post-extraction	Organic post-extraction	5	0.010	–	0.020
4	Raman	500–1500	1st derivative, norm, MC	Organic post-extraction	Organic post-extraction	4	0.006	–	0.013
5	MIR	600–1800	MC	Aqueous	Aqueous post-extraction	3	0.057	0.099	0.139
6	MIR	670–1500	MC	Organic post-extraction	Organic post-extraction	3	0.005	–	0.006

samples in turn, and applying the model to the samples which were left out. Each block contained the three repeat measurements of each sample. The samples with the lowest and highest acid nitric acid concentrations (samples 1 and 10) were included in every calculation, to give a total of eight splits. Root mean square error of cross validation (RMSECV) values were calculated to assess the accuracy of the cross validation predictions when different numbers of latent variables were included in the PLS model. A plot of RMSECV versus number of latent variables was produced and the optimum number of latent variables was chosen from each plot based on where the RMSECV reached a minimum or started to level off.

Initially, mean centring was performed on the MIR spectra, and derivatisation followed by mean centring was performed on the Raman spectra. Derivatisation was necessary to remove baseline offsets in the Raman spectra, and a Savitsky-Golay first derivative with a filter width of 15 and a polynomial order of 2 was used. When these methods of pre-processing were found to be insufficient to produce accurate predictions, a design of experiments approach was used to determine the optimum pre-processing and model building conditions (Flaten and Walmsley, 2003).

To assess the performance of the PLS models, the predicted nitric acid concentration of each test sample was compared to the concentration determined by titration (for the aqueous phase) or calculated (for the organic phase). For the aqueous phase samples, root mean square error of prediction (RMSEP) values were calculated. As no independent test set was available for the organic phase samples, cross validation was used to assess the ability of the model to predict the concentration of samples when excluded from the calibration set and RMSECV values were calculated.

2.4.2. U-TBP/OK-H_2O/HNO_3 model system

For the samples containing uranyl nitrate and nitric acid (detailed in section 2.1.2), PLS models were built to predict the concentration of nitric acid from the spectra. Mean centring and derivatisation were performed before building the models. The first derivative was performed on the MIR spectra and the second derivative was performed on the Raman spectra. The full spectral range was used to build the PLS models for the Raman spectra, and the range 450–1700 cm^{-1} was used for the MIR spectra. As an independent test set was not available for the organic phase samples, cross validation was used to assess the ability of the model to predict the concentration of samples when excluded from the calibration set and RMSECV values were calculated.

3. Results and discussion

3.1. Raman spectroscopy of TBP/OK-H_2O–HNO_3 model system

3.1.1. Aqueous phase

The first derivative of Raman spectra of aqueous phase samples containing 0.5, 3, 6 and 12 M nitric acid (see section 2.1.1) are displayed in Fig. 1. The original spectra are displayed in Fig. S1 of the Supplementary Information. All peak positions quoted refer to the original spectra, and the first derivative of the intensity at these positions is equal to zero. The main peak at 1047 cm^{-1} arises from the nitrate ion (ν_1 symmetric stretch). The intensity of the peak increases with nitric acid concentration up to 6–9 M, then begins to decrease. This is due to the speciation of nitric acid. Below 2 M, nitric acid is fully dissociated and exists in the free nitrate form. At higher concentrations, solvent separated ion pairs begin to form so there is no longer a linear relationship between the intensity of the nitrate peak at 1047 cm^{-1} and nitric acid concentration (Hlushak et al., 2013; Levanov et al., 2017). The solvent separated ion pairs give rise to a peak at 1034 cm^{-1}, which is obscured by the nitrate peak at 1047 cm^{-1} (Hlushak et al., 2013; Levanov et al., 2017; Ruas et al., 2012). Additional peaks at 960 cm^{-1} (attributed to ν N–OH) and 1305 cm^{-1} arise at high concentrations due to the formation of chemical pairs (i.e. molecular nitric acid) (Hlushak et al., 2013; Levanov et al., 2017; Ruas et al., 2012). A small decrease in the intensity of the peak for each sample can be observed upon extraction as the concentration of nitric acid decreases (Fig. 2). Small variations in

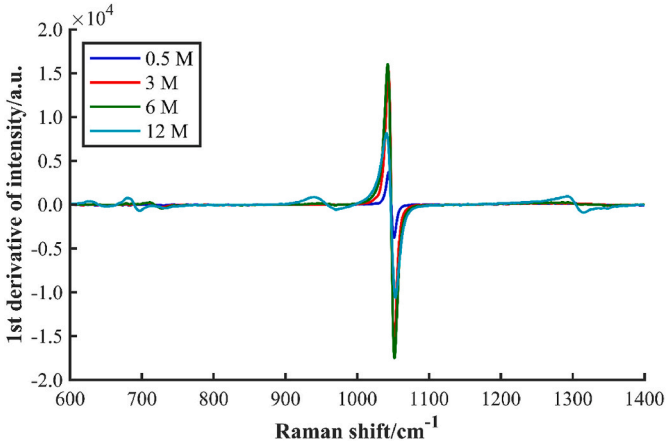

Fig. 1. 1st derivative of Raman spectra of aqueous phase samples containing 0.5, 3, 6 and 12 M nitric acid.

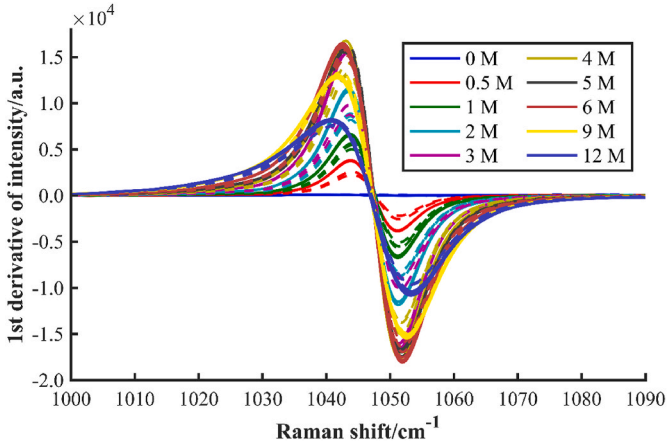

Fig. 2. 1st derivative of the nitrate peak in Raman spectra of aqueous phase samples containing 0–12 M nitric acid. Solid lines = without extraction (concentrations given in Table S1 of the Supplementary Information), dashed lines = after extraction (concentrations given in Table 1).

intensity also occur between some of the repeat measurements of each sample; the intensity in Raman spectroscopy can vary due to other factors in addition to concentration, e.g. positioning of the sample or variations in laser output.

The results of the PLS models built for the prediction of nitric acid concentration are summarised in Table 3. When only the first derivative and mean centring were performed on the Raman spectra of the aqueous phase (PLS model 1), an RMSEP value of 0.627 M was obtained. Predictions were accurate below 2 M, but at higher concentrations they began to deviate. When normalisation was performed in addition (model 2 in Table 3), the RMSEP value decreased to 0.246 M, but deviations from linearity occurred below 1 M, as normalisation introduced noise into the spectra of sample 1. The area of the water peak in the region 2800–3800 cm^{-1} has been used to normalise Raman spectra of nitric acid (Casella et al., 2016; Lines et al., 2018; Nelson et al., 2018), but this peak was outwith the spectral range of the instrument used in the present study. When a combination of models 1 and 2 was used, with model 1 applied to concentrations <2 M and model 2 applied to concentrations ≥2 M, the RMSEP value decreased to 0.148 M and accurate predictions were obtained for all samples. Parity plots showing the predicted versus actual nitric acid concentrations obtained using model 1, model 2 and a combination of models 1 and 2 are shown in Fig. S4 of the Supplementary Information.

An RMSEP value of 0.14 M has been reported in the literature (Nelson et al., 2019) for the quantification of nitric acid in the presence of $Nd(NO_3)_3$ using Raman spectroscopy and PLS, with acid concentrations ranging from 0 to 10 M and a spectral range of 250–4000 cm^{-1}. In the absence of $Nd(NO_3)_3$, an RMSECV value of 0.41 M was reported (Nelson et al., 2018) for the quantification of 0–5 M nitric acid by PLS using a micro-Raman system operating in the range 200–3800 cm^{-1}. In this range, the water peak at 2800–3800 cm^{-1} can be used to normalise the spectra. A similar spectral range has been used to quantify nitric acid over the concentration range 0–6 M in the presence of $Nd(NO_3)_3$ and $NaNO_3$, and an RMSEP value of 0.121 M was obtained (Nee et al., 2018). Raman spectroscopy has also been used to quantify 0–8 M nitric acid in the presence of $NaNO_3$, and RMSEP values of 0.17 M and 0.30 M were obtained for test samples acquired using flow cells of different pathlengths (1 cm and 100 μm respectively, with calibration samples acquired under stationary conditions using 4 cm pathlength vials) (Lines et al., 2018). Therefore, the RMSEP value obtained in this work is comparable to those reported in the literature.

3.1.2. Organic phase

The first derivative of the Raman spectra of the organic phase nitric acid samples prepared by extraction (Table 1) are displayed in Fig. 3 (a), and the original spectra are displayed in Fig. S2 of the Supplementary Information. The majority of the peaks arise from the solvent, but small changes can be observed with increasing acid concentration. The regions in which changes can be observed are shown on an expanded scale in Fig. 3 (b)–(e). The N–OH stretch at 940 cm^{-1} increases in intensity with nitric acid concentration, and small changes in intensity can be observed around 1200 cm^{-1} and at 1310 cm^{-1} due to the NOO stretch (Nelson et al., 2018). In addition, an increase in intensity occurs with nitric acid concentration at 635 and 685 cm^{-1}.

When the first derivative and mean centring were performed (model 3 in Table 3), an RMSECV value of 0.020 M was obtained; however five latent variables were necessary as the spectra were dominated by the solvent. Normalisation to unit length reduced the number of latent variables required to four (model 4 in Table 3), and an RMSECV value of 0.013 M was obtained. This value is around ten times lower than the RMSEP value obtained for the aqueous phase model since the concentration range of the organic phase samples was around an order of magnitude smaller. Parity plots showing the predicted versus actual nitric acid concentrations are shown in Fig. S5 of the Supplementary Information. RMSEC and RMSECV values of 0.05 M have been reported in the literature (Nelson et al., 2018) for the quantification of nitric acid (with concentrations ranging from 0 to 0.8 M) in the organic phase using PLS and Raman spectroscopy. A least squares baseline correction and normalisation were applied. The RMSECV value obtained in this work was around four times lower than that obtained by Nelson et al.

3.2. MIR spectroscopy of TBP/OK-H_2O/HNO_3 model system

3.2.1. Aqueous phase

The MIR spectra of the aqueous phase nitric acid samples (detailed in section 2.1.1) are displayed in Fig. 4. The peaks are broad due to hydrogen bonding, but the absorbance of the peaks between 900 and 1500 cm^{-1} increases with nitric acid concentration. The broad peak at around 1350 cm^{-1} arises from NOO (ν_1 stretch) (Ferraro et al., 2001; McCurdy et al., 2002; Stern et al., 1960). With increasing concentration, this peak shifts to a lower wavenumber (~1300 cm^{-1}) and the shoulder of the peak becomes more pronounced and shifts to a higher wavenumber (~1420 cm^{-1}). An additional peak at around 940 cm^{-1} occurs at high concentration (≥6–9 M), arising from N–OH (ν_2 stretch) (Ferraro et al., 2001; McCurdy et al., 2002; Stern et al., 1960). This is consistent with the formation of molecular nitric acid observed in the Raman spectra at high concentrations. The peak at approximately 1630 cm^{-1} and the very broad peak below 900 cm^{-1} arise from water. For each sample, a decrease in absorbance can be observed upon extraction (solid versus dashed lines) as the acid concentration decreases. For the prediction of nitric acid concentration in the aqueous phase by MIR spectroscopy (model 5 in Table 3 and Fig. S6 (a) in the Supplementary Information), an RMSEP value of 0.099 M could be obtained with no pre-processing other than mean centring. This value was lower than that obtained using Raman spectroscopy, demonstrating that despite the broadness of the peaks, MIR spectroscopy is suitable for detection of nitric acid in the aqueous phase.

3.2.2. Organic phase

The MIR spectra of the organic phase nitric acid samples prepared by extraction (Table 1) are shown in Fig. 5. With increasing nitric acid concentration, the P=O stretch at 1270 cm^{-1} shifted to 1210 cm^{-1}, the NOO stretch at 1307 cm^{-1} increased in absorbance, and changes in the shape of the P–O–C stretch at 950–1100 cm^{-1} could be observed. This is due to the complexation of nitric acid with TBP, and is consistent with the literature (Ferraro et al., 2001). These changes indicate that MIR spectroscopy is suitable for monitoring the extraction of nitric acid into the organic phase.

With no pre-processing other than mean centring (model 6 in Table 3 and Fig. S6 (b) in the Supplementary Information), an RMSECV value of

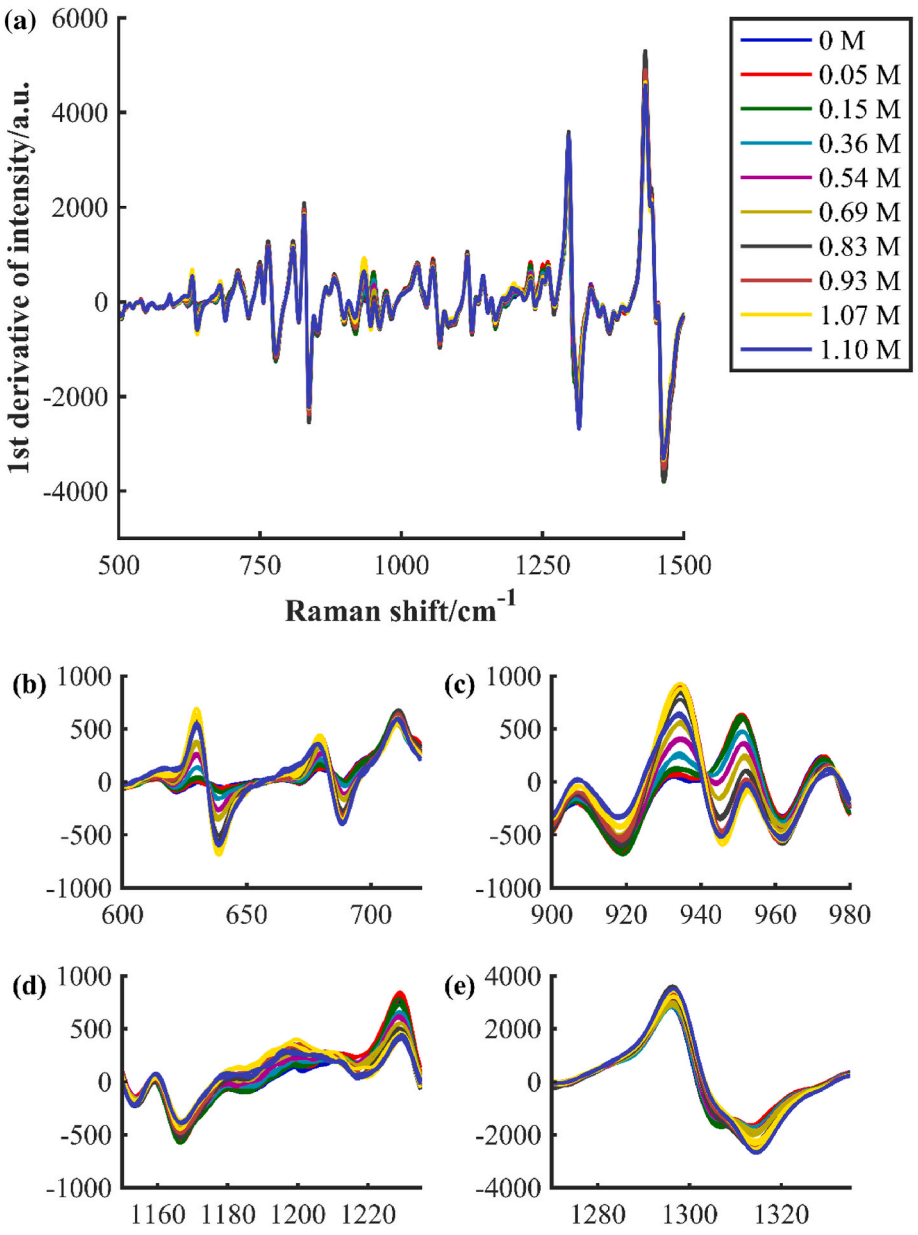

Fig. 3. 1st derivative of Raman spectra of organic phase samples containing 0–1.10 M nitric acid prepared by extraction of nitric acid into 30% v/v TBP in OK, in the spectral regions (a) 500–1500 cm^{-1}, (b) 600–720 cm^{-1}, (c) 900–980 cm^{-1}, (d) 1150–1235 cm^{-1} and (e) 1270–1335 cm^{-1}.

0.006 M was obtained. This value is more than an order of magnitude lower than the RMSEP value obtained for the aqueous phase owing to the lower acid concentration in the organic phase. Additional pre-processing such as application of the first derivative and normalisation to unit length were not necessary. The RMSECV value obtained by MIR spectroscopy is around half that obtained by Raman spectroscopy of the organic phase. This is likely to be because the peaks arising from nitric acid are more easily distinguished from the solvent peaks in the MIR spectra than the Raman spectra.

The RMSECV value obtained for the organic phase in the present study is more accurate than the RMSEP value reported in the literature (Kirsanov et al., 2013) for the prediction of nitric acid concentration in the organic phase using MIR spectra and PLS regression (1.75 g/L or 0.028 M). Kirsanov et al. used 17 samples containing uranium and nitric acid (with acid concentrations ranging from 0.016 to 0.51 M) to build the model, which was applied to 7 independent test samples. Autoscaling was the only method of pre-processing performed; however, derivatisation has also been performed prior to building PLS models for the quantification of TBP and dibutylphosphoric acid by MIR spectroscopy (Levitskaia et al., 2013). The effect of autoscaling on the PLS predictions was investigated in our work but the results obtained were found to be comparable to those obtained using mean centring.

These results demonstrate that both MIR spectroscopy and Raman spectroscopy, in combination with appropriate pre-processing techniques and PLS regression, are suitable for monitoring nitric acid concentration in the aqueous and organic phases during the PUREX process.

3.3. *U-TBP/OK-H_2O–HNO_3 model system*

The ability to predict nitric acid concentration in the aqueous and organic phases of the PUREX-relevant model system TBP/OK-H_2O–HNO_3 has been demonstrated. However, other species present in the PUREX process such as uranyl nitrate may impact the predictions. To assess the effect of uranyl nitrate on the spectra of nitric acid, example first derivative Raman and MIR spectra of organic phase samples containing the same concentration of nitric acid (0.6 M) with and without

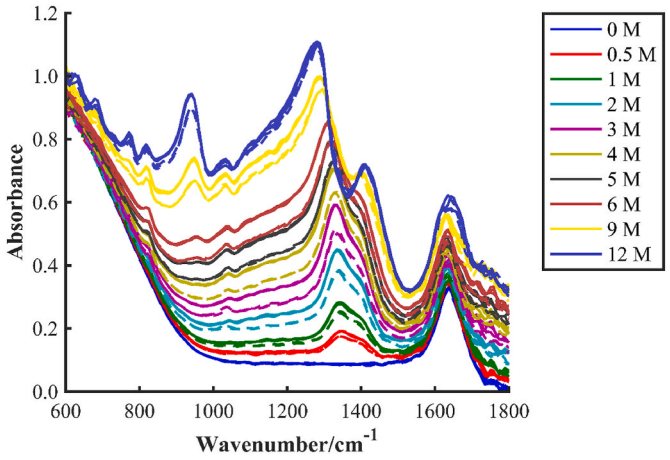

Fig. 4. MIR spectra of aqueous phase samples containing 0–12 M nitric acid. Solid lines = without extraction (concentrations given in Table S1 of the Supplementary Information), dashed lines = after extraction (concentrations given in Table 1).

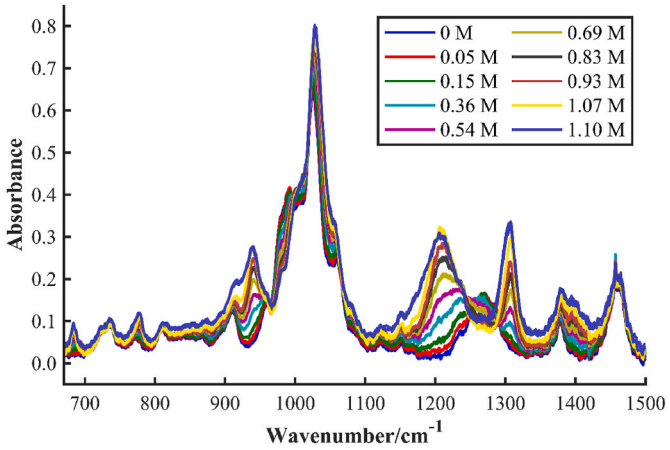

Fig. 5. MIR spectra of organic phase samples containing 0–1.10 M nitric acid prepared by extraction of nitric acid into 30% v/v TBP in OK.

uranyl nitrate are displayed in Fig. 6. The original spectra are displayed in Fig. S3 of the Supplementary Information. The presence of uranium gives rise to two additional peaks in the Raman spectrum, at 860 and 1030 cm^{-1}. The peak at 860 cm^{-1} arises from UO_2^{2+} (ν_1 symmetric stretch) and the peak at 1030 cm^{-1} arises from uranyl-bound nitrate (ν_4 frequency) (Bryan et al., 2011a, 2011b). In the MIR spectra, uranium produces additional peaks at 940 and 1525 cm^{-1}, and a shift of the P=O band to 1190 cm^{-1} (Borkowski et al., 2002; Chiarizia et al., 2003). The peak at 940 cm^{-1} arises from the UO_2^{2+} stretch and the peak at 1525 cm^{-1} can be attributed to the ONO stretch of a nitrate group chelated to a metal (Borkowski et al., 2002; Chiarizia et al., 2003). Therefore, it is possible to distinguish the spectra of nitric acid and uranyl nitrate in the organic phase using both techniques.

When PLS was performed to predict the nitric acid concentration in the presence of uranium, RMSECV values of 0.066 and 0.027 M were obtained for Raman and MIR spectroscopy respectively. Four latent variables were required for the Raman model (RMSEC of 0.021 M) and two latent variables were required for the MIR model (RMSEC of 0.015 M). Parity plots showing the predicted versus actual nitric acid concentrations are shown in Fig. S7 of the Supplementary Information. The RMSECV values obtained were higher than for the samples without uranium (Table 3) due to extra variation in the spectra and reference values arising from the experimental approach. The variation in TBP

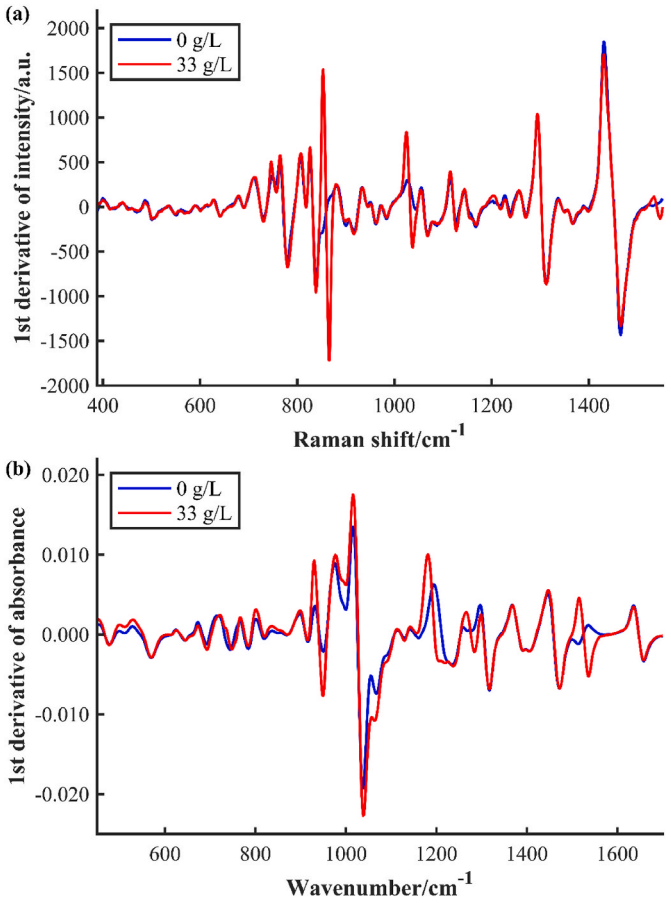

Fig. 6. 1st derivative of (a) Raman and (b) MIR spectra of organic phase samples containing 0.6 M nitric acid with 0 g U/L uranium (in the form $UO_2(NO_3)_2$) in 30% v/v TBP (blue) and 33 g U/L uranium in 35% v/v TBP (red).

concentration may also have reduced the accuracy of the predictions. As uranium was present in addition to nitric acid, normalisation of the spectra to unit length could not be performed. If a Raman spectrometer capable of measuring a larger spectral range was used, the spectra could be normalised to the area of the water peak (Casella et al., 2016; Lines et al., 2018; Nelson et al., 2018), which may improve the accuracy of the predictions in the presence of uranium. However, it is evident that the concentration of nitric acid can still be predicted in samples of the organic phase containing uranyl nitrate.

4. Conclusions

The ability of MIR and Raman spectroscopy to accurately measure nitric acid concentration in both the aqueous and organic phases of PUREX-relevant samples has been demonstrated. The Raman spectra were more complex than the MIR spectra due to the effect of acid speciation, and the organic phase was more complex than the aqueous phase as the spectra were dominated by the solvent. However, the predictions were improved by the application of pre-processing techniques such as derivatisation and normalisation, and were more accurate than those reported in the literature for models built using larger spectral ranges or smaller concentration ranges (which might be expected to produce more accurate results). For each phase, accurate predictions of nitric acid concentration could be obtained using both techniques, with MIR spectroscopy producing lower RMSE values than Raman (RMSEP values of 0.099 M versus 0.148 M for the aqueous phase and RMSECV values of 0.006 M versus 0.013 M for the organic phase of the TBK/OK-H_2O–HNO_3 model system). Accurate predictions of nitric

acid concentration in the organic phase could also be obtained in the presence of uranyl nitrate for the U-TBK/OK-H_2O–HNO_3 model system (RMSECV values of 0.027 and 0.066 M for MIR and Raman spectroscopy, respectively). Both MIR and Raman spectroscopy are, therefore, suitable for off-line monitoring of nitric acid concentration in PUREX-relevant mixtures as an alternative to titration. The use of optical spectroscopy to quantify nitric acid concentration will increase the speed of measurements compared to titration and will reduce the amount of waste generated. In addition, MIR and Raman spectroscopy could be used for on-line monitoring of nitric acid concentration during the PUREX process. This will eliminate the need for extractive sampling and enable the acquisition of real-time measurements for process monitoring and process control, including ultimately the potential for real-time accountancy to support advanced safeguarding of future nuclear materials processing.

Declaration of competing interest

The authors declare that they have no known competing financial interests or personal relationships that could have appeared to influence the work reported in this paper.

Data availability

All data underpinning this publication are openly available from the University of Strathclyde KnowledgeBase at https://doi.org/10.15129/58c05738-4b8d-4fe3-8803-24a2321cf7fb.

Acknowledgements

This work was funded under the £46m Advanced Fuel Cycle Programme (AFCP) as part of the Department for Business, Energy and Industrial Strategy's (BEIS) £505m Energy Innovation Programme. A National Nuclear Laboratory (NNL) User Access award, supported by AFCP, enabled the sample preparation and spectroscopic analysis of the uranyl nitrate and nitric acid samples detailed in section 2.1.2 to be performed at NNL.

Appendix A. Supplementary data

Supplementary data to this article can be found online at https://doi.org/10.1016/j.pnucene.2023.104898.

References

Arrigo, L.M., Christensen, R.N., Fraga, C.G., Liezers, M., Peper, S.M., Thomas, E.M., Bryan, S.A., Douglas, M., Laspe, A.R., Lines, A.M., Peterson, J.M., Ward, R.M., Casella, A.J., Duckworth, D.C., Levitskaia, T.G., Orton, C.R., Schwantes, J.M., 2009. FY 2009 Progress: Process Monitoring Technology Demonstration at PNNL. Pacific Northwest National Laboratory (PNNL), Richland, WA (United States).

Asmussen, S.E., Lines, A.M., Bottenus, D., Heller, F., Bryan, S.A., Delegard, C., Louie, C., Lumetta, G., Pellegrini, K., Pitts, W.K., Clark, S., Casella, A., 2019. In situ monitoring and kinetic analysis of the extraction of nitric acid by tributyl phosphate in n-dodecane using Raman spectroscopy. Solvent Extr. Ion Exch. 37, 157–172.

Balasubramonian, S., Srivastav, R.K., Kumar, S., Sivakumar, D., Sinha, P.K., Sampath, M., Mudali, U.K., 2013. Speciation of 30 % tri-n-butyl phosphate solvent during extraction of nitric acid. J. Radioanal. Nucl. Chem. 295, 1703–1707.

Borkowski, M., Ferraro, J.R., Chiarizia, R., McAlister, D.R., 2002. FT-IR study of third phase formation in the U(VI) or Th(IV)/HNO_3, TBP/alkane systems. Solvent Extr. Ion Exch. 20, 313–330.

Bryan, S.A., Levitskaia, T.G., Casella, A.J., 2014. On-line Monitoring for Process Control and Safeguarding of Radiochemical Streams at Spent Fuel Reprocessing Plants. Pacific Northwest National Laboratory (PNNL), Richland, WA (United States).

Bryan, S.A., Levitskaia, T.G., Casella, A.J., Peterson, J.M., Johnsen, A.M., Lines, A.M., Thomas, E.M., 2011a. Spectroscopic on-line monitoring for process control and safeguarding of radiochemical streams in nuclear fuel reprocessing facilities. In: Nash, K.L., Lumetta, G.J. (Eds.), Advanced Separation Techniques for Nuclear Fuel Reprocessing and Radioactive Waste Treatment. Woodhead Publ. Ltd, Cambridge, pp. 95–119.

Bryan, S.A., Levitskaia, T.G., Johnsen, A.M., Orton, C.R., Peterson, J.M., 2011b. Spectroscopic monitoring of spent nuclear fuel reprocessing streams: an evaluation of spent fuel solutions via Raman, visible, and near-infrared spectroscopy. Radiochim. Acta 99, 563–571.

Bryan, S.A., Levitskaia, T.G., Schwantes, J.M., Orton, C.R., Peterson, J.M., Casella, A.J., 2011c. Monitoring, controlling and safeguarding radiochemical streams at spent fuel reprocessing facilities, Part 1: optical spectroscopic methods. Int. J. Nucl. Energy Manag. Saf. 1, 21–38.

Casella, A., Lines, A., Nelson, G., Bello, J., Bryan, S., 2016. MicroRaman measurements for nuclear fuel reprocessing applications. Atalante 2016 Int. Conf. Nuclear Chem. Sustain. Fuel Cycles 21, 466–472.

Casella, A.J., Levitskaia, T.G., Peterson, J.M., Bryan, S.A., 2013. Water O-H stretching Raman signature for strong acid monitoring via multivariate analysis. Anal. Chem. 85, 4120–4128.

Chen, H.Y., Taylor, R., Jobson, M., Woodhead, D., Masters, A., 2016. Development and validation of a flowsheet simulation model for neptunium extraction in an advanced PUREX process. Solvent Extr. Ion Exch. 34, 297–321.

Chiarizia, R., Jensen, M.P., Borkowski, M., Ferraro, J.R., Thiyagarajan, P., Littrell, K.C., 2003. Third phase formation revisited: the U(VI), HNO_3-TBP, n-dodecane system. Solvent Extr. Ion Exch. 21, 1–27.

Davis, W., Debruin, H.J., 1964. New activity coefficients of 0-100 per cent aqueous nitric acid. J. Inorg. Nucl. Chem. 26, 1069–1083.

Debus, B., Kirsanov, D., Ruckebusch, C., Agafonova-Moroz, M., Babain, V., Lumpov, A., Legin, A., 2015. Restoring important process information from complex optical spectra with MCR-ALS: case study of actinide reduction in spent nuclear fuel reprocessing. Chemometr. Intell. Lab. Syst. 146, 241–249.

Ferraro, J.R., Borkowski, M., Chiarizia, R., McAlister, D.R., 2001. FT-IR spectroscopy of nitric acid in TBP/octane solution. Solvent Extr. Ion Exch. 19, 981–992.

Flaten, G.R., Walmsley, A.D., 2003. Using design of experiments to select optimum calibration model parameters. Analyst 128, 935–943.

Herbst, R.S., Baron, P., Nilsson, M., 2011. Standard and advanced separation: PUREX processes for nuclear fuel reprocessing. In: Nash, K.L., Lumetta, G.J. (Eds.), Advanced Separation Techniques for Nuclear Fuel Reprocessing and Radioactive Waste Treatment. Woodhead Publ Ltd, Cambridge, pp. 141–175.

Hlushak, S., Simonin, J.P., De Sio, S., Bernard, O., Ruas, A., Pochon, P., Jan, S., Moisy, P., 2013. Speciation in aqueous solutions of nitric acid. Dalton Trans. 42, 2853–2860.

Kirsanov, D., Babain, V., Agafonova-Moroz, M., Lumpov, A., Legin, A., 2013. Approach to on-line monitoring of PUREX process using chemometric processing of the optical spectral data. Radiochim. Acta 101, 149–154.

Lefebvre, C., Dumas, T., Tamain, C., Ducres, T., Solari, P.L., Charbonnel, M.C., 2017. Addressing ruthenium speciation in tri-n-butyl-phosphate solvent extraction process by Fourier transform infrared, extended X-ray absorption fine structure, and single crystal X-ray diffraction. Ind. Eng. Chem. Res. 56, 11292–11301.

Levanov, A.V., Isaikina, O.Y., Lunin, V.V., 2017. Dissociation constant of nitric acid. Russ. J. Phys. Chem. A 91, 1221–1228.

Levitskaia, T.G., Peterson, J.M., Campbell, E.L., Casella, A.J., Peterman, D.R., Bryan, S. A., 2013. Fourier transform infrared spectroscopy and multivariate analysis for online monitoring of dibutyl phosphate degradation product in tributyl phosphate/n-dodecane/nitric acid solvent. Ind. Eng. Chem. Res. 52, 17607–17617.

Lines, A.M., Nelson, G.L., Casella, A.J., Bello, J.M., Clark, S.B., Bryan, S.A., 2018. Multivariate analysis to quantify species in the presence of direct interferents: micro-Raman analysis of HNO_3 in microfluidic devices. Anal. Chem. 90, 2548–2554.

Liu, Y.Q.C., Dunn, D., Lipari, M., Barton, A., Firth, P., Speed, J., Wood, D., Nagy, Z.K., 2019. A comparative study of continuous operation between a dynamic baffle crystallizer and a stirred tank crystallizer. Chem. Eng. J. 367, 278–294.

May, I., Taylor, R.J., Denniss, I.S., Wallwork, A.L., 1999. Actinide complexation in the PUREX process. Czech. J. Phys. 49, 597–601.

McCurdy, P.R., Hess, W.P., Xantheas, S.S., 2002. Nitric acid-water complexes: theoretical calculations and comparison to experiment. J. Phys. Chem. A 106, 7628–7635.

McLachlan, F., Greenough, K., Geist, A., McLuckie, B., Modolo, G., Wilden, A., Taylor, R., 2016. Nitric acid extraction into the TODGA/TBP solvent. Solvent Extr. Ion Exch. 34, 334–346.

Nee, K., Bryan, S.A., Levitskaia, T.G., Kuo, J.W.J., Nilsson, M., 2018. Combinations of NIR, Raman spectroscopy and physicochemical measurements for improved monitoring of solvent extraction processes using hierarchical multivariate analysis models. Anal. Chim. Acta 1006, 10–21.

Nelson, G.L., Asmussen, S.E., Lines, A.M., Casella, A.J., Bottenus, D.R., Clark, S.B., Bryan, S.A., 2018. Micro-Raman technology to interrogate two-phase extraction on a microfluidic device. Anal. Chem. 90, 8345–8353.

Nelson, G.L., Lines, A.M., Bello, J.M., Bryan, S.A., 2019. Online monitoring of solutions within microfluidic chips: simultaneous Raman and UV-Vis absorption spectroscopies. ACS Sens. 4, 2288–2295.

Orton, C.R., Bryan, S.A., Casella, A.J., Hines, W., Levitskaia, T.G., Henkell, J.J., Schwantes, J.M., Jordan, E.A., Lines, A.M., Fraga, C.G., Peterson, J.M., Verdugo, D. E., Christensen, R.N., Peper, S.M., 2011. FY-2010 Process Monitoring Technology Final Report. Pacific Northwest National Laboratory (PNNL), Richland, WA (United States).

Rodriguez-Ruiz, I., Lamadie, F., Charton, S., 2018. Uranium(VI) on-chip microliter concentration measurements in a highly extended UV-visible absorbance linearity range. Anal. Chem. 90, 2456–2460.

Ruas, A., Pochon, P., Hlushak, S., Simonin, J.P., Bernard, O., Moisy, P., 2012. Speciation in aqueous solutions of nitric acid estimated within the binding mean spherical approximation (BiMSA). Atalante 2012 International Conference on Nuclear Chemistry for Sustainable Fuel Cycles 7, 374–379.

Schwantes, J.M., Bryan, S.A., Orton, C.R., Levitskaia, T.G., Pratt, S.H., Fraga, C.G., Coble, J.B., 2012. Advanced process monitoring safeguards technologies at pacific northwest national laboratory. Atalante 2012 Int. Conf. Nuclear Chem. Sustain. Fuel Cycles 7, 716–724.

Stern, S.A., Mullhaupt, J.T., Kay, W.B., 1960. The physicochemical properties of pure nitric acid. Chem. Rev. 60, 185–207.
Taylor, R.J., Gregson, C.R., Carrott, M.J., Mason, C., Sarsfield, M.J., 2013. Progress towards the full recovery of neptunium in an advanced PUREX process. Solvent Extr. Ion Exch. 31, 442–462.
Verma, P.K., Mohapatra, P.K., Bhattacharyya, A., Yadav, A.K., Jha, S.N., Bhattacharyya, D., 2018. Structural investigations on uranium(VI) and thorium(IV) complexation with TBP and DHOA: a spectroscopic study. New J. Chem. 42, 5243–5255.